Breathing-like excited state of the Hoyle state in ^{12}C

Bo Zhou,[1,2,*] Akihiro Tohsaki,[3] Hisashi Horiuchi,[3,4] and Zhongzhou Ren[5,6,7]
[1]*Institute for International Collaboration, Hokkaido University, Sapporo 060-0815, Japan*
[2]*Faculty of Science, Hokkaido University, Sapporo 060-0810, Japan*
[3]*Research Center for Nuclear Physics (RCNP), Osaka University, Osaka 567-0047, Japan*
[4]*International Institute for Advanced Studies, Kizugawa 619-0225, Japan*
[5]*Department of Physics, Nanjing University, Nanjing 210093, China*
[6]*Center of Theoretical Nuclear Physics, National Laboratory of Heavy-Ion Accelerator, Lanzhou 730000, China*
[7]*Key Laboratory of Theoretical Physics, Institute of Theoretical Physics, Chinese Academy of Sciences, Beijing 100190, China*
(Received 7 July 2016; published 21 October 2016)

The existence of the 0_3^+ and 0_4^+ states around 10 MeV excitation energy in ^{12}C is confirmed by a fully microscopic 3α cluster model. Firstly, a generator coordinate method (GCM) calculation is performed by superposing optimized $2\alpha + \alpha$ Tohsaki-Horiuchi-Schuck-Röpke (THSR) wave functions with the radius-constraint method. The obtained two excited 0^+ states above the Hoyle state are consistent with the recently observed states by experiment. Secondly, a variational calculation using the single $2\alpha + \alpha$ THSR wave function orthogonalized to the ground and Hoyle states is made and it also supports the existence of the 0_3^+ state obtained by the GCM calculation. The analysis of the obtained 0_3^+ state is made by studying its 2α-α reduced width amplitude, its 2α correlation function, and the large monopole matrix element between this state and the Hoyle state, which shows that this 0_3^+ state is a breathing-like excited state of the Hoyle state. This character of the 0_3^+ state is very different from the 0_4^+ state which seems to have a bent-arm 3α structure.

DOI: 10.1103/PhysRevC.94.044319

As one of the universal phenomena in nature, resonance states widely appear in a large variety of fields from particle physics to the condensed matter physics [1]. Systems with electrons, hadrons, or atoms display various and rich resonance states in different ways, which often leads to a new state finding and deepen our understanding for the many-body dynamics. In nuclear physics, due to the complex and special nucleon-nucleon interaction, resonance states are highly common and important in almost all the nuclear systems [2–5]. As one of most important nuclei in nuclear cluster physics, ^{12}C has been studied for a long time especially for the famous Hoyle state [6], which is a narrow 3α resonance state and plays a key role in the synthesis of carbon in the universe. In the past decade, it was surprising to find that there were quite impressive discoveries and new understanding in this old subject, e.g., many new cluster states above the 3α threshold energy were found from experiments such as the new 0_3^+, 0_4^+ [7], 2_2^+ [8], and 4_2^+ [9] states. These observed broad cluster resonance states are expected to provide us with new clues for understanding the Hoyle state. Actually, as we see in this paper, the 0_3^+ resonance state is intimately related to the Hoyle state.

About 40 years ago, the generator coordinate method (GCM) calculation with the 3α Brink wave function by Uegaki *et al.* [10], which reproduced the ground and Hoyle states, gave the 0_3^+ state at $E_x = 11.7$ MeV and assigned it to the observed 0_3^+ state at $E_x = 10.5$ MeV. Later calculations including the antisymmetrized molecular dynamics (AMD) [11] and fermionic molecular dynamics (FMD) [12] also gave the 0_3^+ state around $E_x = 10$ MeV. All the 0_3^+ states by these calculations have a characteristic feature that they contain a nonsmall component of $^8\mathrm{Be}(2^+) + \alpha$ (D-wave) configuration. In AMD and FMD, this feature has been referred to as the bent-arm structure of 3α. However, about ten years ago Kurokawa and Katō reported that the 3α orthogonality condition model (OCM) calculation combined with the complex scaling method (CSM) gives another 0^+ state [13] around $E_x = 10$ MeV in addition to the 0^+ state with the bent-arm–like structure of 3α. This new 0^+ state has 2α-α reduced width amplitude whose node number is larger than that of the Hoyle state. The existence of two 0^+ states around $E_x = 10$ MeV was soon later supported by Itoh *et al.* [7] experimentally who showed that the broad 0_3^+ state at $E_x = 10.5$ MeV is divided into two 0^+ states, namely 0_3^+ and 0_4^+ states at 9.04 MeV and 10.56 MeV with the widths of 1.45 MeV and 1.42 MeV, respectively. Itoh *et al.* reported that the 0_3^+ state decays dominantly through the $^8\mathrm{Be}(0^+) + \alpha$ (S-wave) channel while the 0_4^+ state decays through the $^8\mathrm{Be}(2^+) + \alpha$ (D-wave) channel. Thus, the 0_4^+ state corresponds to the 0_3^+ state by Uegaki, AMD, and FMD. The existence of 0_3^+ and 0_4^+ states around 10 MeV was reported by another 3α OCM calculation combined with CSM a few years ago [14] and also by a microscopic 3α model calculation last year [15].

To describe the complex relative motion of clusters in nuclei, OCM as a semimicroscopic cluster model [16], adopts the effective local potential from the nonlocal potential of the resonating group method (RGM) in an approximate way, and the (almost) forbidden sates are removed using some projection operator. Different from this simple treatment in OCM, the microscopic cluster model adopts the effective nucleon-nucleon interaction [17,18] and also the fully antisymmetrized effects are considered. By fully taking into account the Pauli principle between all the constituent nucleons, the microscopic cluster model [19] provides us with a very

*bo@nucl.sci.hokudai.ac.jp.

powerful and reliable tool for studying the clusters in nuclei. A microscopic 3α model calculation is especially important for examining the existence of 0_3^+ and 0_4^+ states around 10 MeV because both AMD and FMD calculations have reported only the existence of the 0_4^+ state. It is therefore highly desirable to perform another microscopic 3α model calculation in order to confirm the existence of 0_3^+ and 0_4^+ states around 10 MeV and also to clarify the character of the 0_3^+ state which is far more unknown than that of the 0_4^+ state.

As a novel microscopic cluster wave function, the Tohsaki-Horiuchi-Schuck-Röpke (THSR) wave function has been very successful for the description of the ground state, the ordinary cluster state, and the α-condensate state [20–22]. Especially for some well-developed or gas-like cluster states like Hoyle state in ^{12}C, the jj-coupling shell model components or noncentral interactions are usually very small while the relative motion of clusters is becoming a more important freedom. In this case, the THSR, as a pure cluster wave function, has a natural sort of advantage for describing this kind of cluster freedom due to its α-cluster assumption and nonlocalized character. On the other hand, some other microscopic cluster models, such as the Brink model, AMD, and FMD, sometimes demand large efforts to describe the dilute gas-like cluster state. Quite recently, based on the concept of nonlocalized clustering [21,23], we proposed an extended THSR wave function with 2α correlation, which provides us a more suitable basis for the description of various cluster structures in ^{12}C [24]. Moreover, to deal with the broad resonance state, we use the radius-constraint method [25] as the bound-state approximation and we also develop an improved GCM method for selecting the optimum basis in the practical calculations. Finally, we aim to confirm and investigate the excited 0_3^+ and 0_4^+ states of ^{12}C using the extended THSR wave function as basis wave functions in the improved GCM calculation.

We begin with the extended THSR wave function of Ref. [24], which includes the 2α correlation in 3α cluster structure is written as

$$\Phi(\boldsymbol{\beta}_1,\boldsymbol{\beta}_2) = \int d^3R_1 d^3R_2 \exp\left[-\sum_{i=1}^{2}\left(\frac{R_{ix}^2}{\beta_{ix}^2}+\frac{R_{iy}^2}{\beta_{iy}^2}+\frac{R_{iz}^2}{\beta_{iz}^2}\right)\right]\Phi^B(\boldsymbol{R}_1,\boldsymbol{R}_2) \tag{1}$$

$$\propto \phi_G \mathcal{A}\left\{\exp\left[-\sum_{i=1}^{2}\left(\frac{\xi_{ix}^2}{B_{ix}^2}+\frac{\xi_{iy}^2}{B_{iy}^2}+\frac{\xi_{iz}^2}{B_{iz}^2}\right)\right]\phi(\alpha_1)\phi(\alpha_2)\phi(\alpha_3)\right\}. \tag{2}$$

Here, $B_{1k}^2 = b^2+\beta_{1k}^2$, $B_{2k}^2 = \frac{3}{4}b^2+\beta_{2k}^2$, and $\boldsymbol{\beta}_i \equiv (\beta_{ix},\beta_{iy},\beta_{iz})$. $\boldsymbol{\xi}_1 = \boldsymbol{X}_2 - \boldsymbol{X}_1$, $\boldsymbol{\xi}_2 = \boldsymbol{X}_3 - (\boldsymbol{X}_1+\boldsymbol{X}_2)/2$. $\Phi^B(\boldsymbol{R}_1,\boldsymbol{R}_2)$ is the Brink wave function of ^{12}C. $\boldsymbol{R}_1$ and $\boldsymbol{R}_2$ are the corresponding intercluster distance generator coordinates. ϕ_G is the center-of-mass wave function of ^{12}C, which can be expressed as $\exp(-6X_G^2/b^2)$. In practical calculations, we assume the axial symmetry for the $2\alpha+\alpha$ system, namely, $\boldsymbol{\beta}_i \equiv (\beta_{ix}=\beta_{iy},\beta_{iz})$ $(i=1,2)$. As for the effective nucleon-nucleon interaction, we adopt the Volkov No. 2 force (modified version) with Majorana parameter $M=0.59$ and $b=1.35$ fm, which were used by Kamimura *et al.* for the 3α RGM calculation [26].

Different from the original one-$\boldsymbol{\beta}_0$ 3α THSR wave function [20,27], the $2\alpha+\alpha$ THSR wave function in Eq. (1) introduced two deformed size parameters $\boldsymbol{\beta}_1$ and $\boldsymbol{\beta}_2$. In the 3α cluster system of ^{12}C, 2α clusters make the motion in a container confined by the size parameter $\boldsymbol{\beta}_1$ and this 2α cluster and the third α cluster can be considered to move in the other $\boldsymbol{\beta}_2$-size container. In this way, the 2α correlation has been included in the constructed $2\alpha+\alpha$ THSR wave function. If we make the replacement, $\boldsymbol{\beta}_1 \to \sqrt{2}\boldsymbol{\beta}_0$ and $\boldsymbol{\beta}_2 \to \sqrt{3/2}\boldsymbol{\beta}_0$ in Eq. (1), this extended $2\alpha+\alpha$ THSR wave function just becomes the original one-$\boldsymbol{\beta}_0$ 3α THSR wave function [27].

As we know, to describe the broad resonance cluster states in ^{12}C, the GCM bound-state approximation is no longer available due to the contamination of the continuum states above the threshold energy. To remove the contamination, we used the radius-constraint method (RCM) [22,25] combined with the GCM. We diagonalize the squared radius operator and obtain the corresponding eigenstates and eigenvalues. Since the larger squared radius eigenvalues indicate the continuum states are involved, we adopt the radius eigenfunctions whose eigenvalues are smaller than the cutoff parameter $R_{\rm cut}$ in the GCM calculations. This kind of treatment is very similar to the shell model calculations for resonance states where nucleon orbits are confined within some radial region.

In GCM calculations, a very large basis is necessary for covering various cluster model spaces for the excited 0^+ states of ^{12}C. However, considering the numerical errors from GCM combined with radius-constraint method, it is not suitable to superpose directly a huge number of, e.g., more than 1000, THSR wave functions. In this situation, we propose a way for selecting more effective wave functions as the basis. The steps for this one-by-one GCM+RCM are as follows:

(1) We choose a large number of projected normalized 0^+ THSR wave functions $\{\hat{\Phi}_1^{0^+},\hat{\Phi}_2^{0^+},\ldots,\hat{\Phi}_{2592}^{0^+}\}$ as our prepared basis, which correspond 2592 different sets of mesh points for $(\boldsymbol{\beta}_1,\boldsymbol{\beta}_2)$. The matrix elements of norm, squared radius operator, and Hamiltonian are calculated and prepared for the following calculations. Since the direct diagonalization of Hamiltonian using this huge prepared basis is very difficult, we plan to pick a small number of effective wave functions one by one from the prepared basis for obtaining converged binding energies and wave functions for the ground state and excited 0^+ states of ^{12}C.

(2) At the beginning, we focus on the ground state of ^{12}C and we begin with the first effective wave function among the prepared basis. Firstly, we calculate the binding energies of

single wave functions in the prepared basis. As for calculations by the single wave function $\hat{\Phi}_i^{0^+}$ in GCM+RCM, it simply means if $\sqrt{\langle\hat{\Phi}_i^{0^+}|\sum_k(\boldsymbol{r}_k-\boldsymbol{r}_{\rm cm})^2/12|\hat{\Phi}_i^{0^+}\rangle} > R_{\rm cut}$, the wave function $\hat{\Phi}_i^{0^+}$ will be abandoned, otherwise we retain this wave function and calculate its binding energy. Secondly, if some wave function like $\hat{\Phi}_{233}^{0^+}$ can give the deepest binding energy for the ground state among the prepared basis, then $\hat{\Phi}_{233}^{0^+}$ will be our first selected wave function. It should be noted, to obtain the converged value of the ground state, the pure and traditional GCM is enough and RCM is not necessary since the bound state is almost independent of the parameter $R_{\rm cut}$ in RCM.

(3) Next, we need to choose the second effective wave function among the prepared basis for the ground state of ^{12}C. Assume the first selected wave function is $\hat{\Phi}_{233}^{0^+}$, we then make the diagonalization of the Hamiltonian for all the superposed two wave functions, $\{\hat{\Phi}_{233}^{0^+}+\hat{\Phi}_1^{0^+}\},\{\hat{\Phi}_{233}^{0^+}+\hat{\Phi}_2^{0^+}\},\ldots,\{\hat{\Phi}_{233}^{0^+}+\hat{\Phi}_{2592}^{0^+}\}$ using GCM+RCM. For each $\hat{\Phi}_{233}^{0^+}+\hat{\Phi}_i^{0^+}(i\neq 233)$ we diagonalize the squared radius operator and we retain only the eigenfunctions whose eigenvalues are smaller than $R_{\rm cut}^2$. If the $\{\hat{\Phi}_{233}^{0^+}+\hat{\Phi}_{737}^{0^+}\}$ group can give the deepest energy for the ground state, then we can choose $\hat{\Phi}_{737}^{0^+}$ as our second selected wave function. One by one, we can obtain dozens of very effective wave functions (e.g., 50) for the ground state and the corresponding eigenvalue has been very well converged. Here we emphasize again, as for the selected n_B 0^+ THSR wave functions from the prepared basis in the GCM+RCM calculations, the adopted radius eigenfunctions should have smaller ($\leqslant R_{\rm cut}$) eigenvalues while each of these radius eigenfunctions is a linear combination of the selected n_B 0^+ THSR wave functions. In addition, in the selection process, the wave functions bringing fluctuation and large numerical errors for the excited 0^+ states will also be abandoned.

(4) After selecting 50 effective wave functions for the ground state, in the same way, we continue to choose more effective wave functions for the 0_2^+, 0_3^+, and 0_4^+ states in ^{12}C in turn. Namely we select additional effective wave functions so that we get deeper binding energies for the 0_2^+, 0_3^+, and 0_4^+ states. Finally, after selecting lots of wave functions with the fixed parameter $R_{\rm cut}$, e.g., the maximum number is around 70 for $R_{\rm cut}=6$ fm, we cannot select any wave functions from the prepared basis for meeting our requirements, then the selection process is completed.

The one-by-one method is a very effective and general approach for selecting the good basis in the GCM calculation, especially for some kinds of resonance states with large model spaces. Figure 1 shows the GCM-THSR results for the first four 0^+ states of ^{12}C using different values of the radius cut-off parameter $R_{\rm cut}$ in the radius-constraint method. The basis wave functions are constructed from 2592 THSR wave functions [2592 mesh points for $(\beta_{1x},\beta_{1z},\beta_{2x},\beta_{2z})$]. It is known that the ground state of ^{12}C is a compact bound cluster state and the Hoyle state around the 3α threshold energy has a very narrow width of only 8.5 eV, which can be seen as a weakly bound state. In Fig. 1, it can be seen that the ground state and the Hoyle state in GCM calculations are almost independent of the $R_{\rm cut}$ parameter. The energies of the two states reach their converged values already at the small number of basis states. We need to notice that by using the constructed basis, dozens

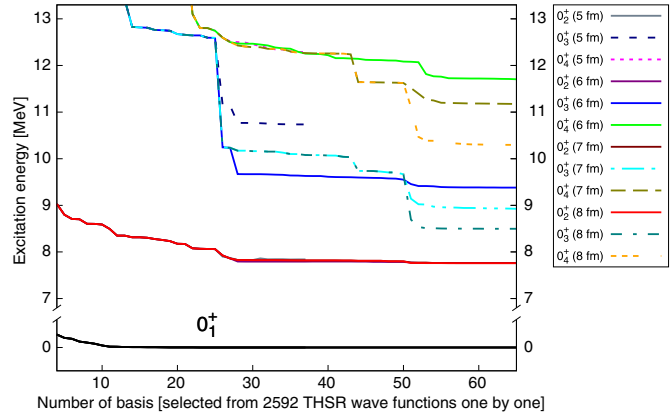

FIG. 1. GCM-THSR results for the ground and three excited 0^+ states of ^{12}C using different values of the cut-off parameter $R_{\rm cut}$ in the radius-constraint method. The values of the cut-off parameter $R_{\rm cut}$ are shown in $0_k^+(R_{\rm cut})$ in the insert. The excitation energies are relative to the obtained GCM converged energy for the ground state -89.65 MeV [24].

of superposed wave functions rather than hundreds of them can give a very exact converged solution compared with the traditional GCM calculations.

As for the broad excited 0^+ states, the choice of the $R_{\rm cut}$ parameter should be careful. The smaller $R_{\rm cut}$ ($\leqslant$5 fm) can lead to a miss of some important model spaces while too large $R_{\rm cut}$ ($\geqslant$9 fm) will bring obvious contamination from the continuum states. The obtained GCM energies of the 0_3^+ and 0_4^+ states for $R_{\rm cut}=6$ fm are seen to be almost constant against the increase of the number of basis states n_B in the region of $n_B>30$ for the 0_3^+ state and $n_B>40$ for the 0_4^+ state. The constancy of the GCM energy against the increase of n_B is a little worse for the 0_4^+ state than for the 0_3^+ state, but still the constancy of the 0_4^+ state energy is within the range of about 0.5 MeV. The GCM energies of these 0^+ states for larger $R_{\rm cut}=7$ fm and 8 fm change their values against the increase of n_B although the amount of change is not so large. These behaviors of the 0_3^+ and 0_4^+ energies for $R_{\rm cut}=7$ fm and 8 fm mean that the GCM wave functions for $R_{\rm cut}=7$ fm and 8 fm contain the contamination of continuum state components. Thus we conclude that the GCM results for $R_{\rm cut}=6$ fm shown in Fig. 1 give the converged results for the energies and wave functions of the 0_3^+ and 0_4^+ states. The converged energies 9.38 MeV and 11.7 MeV of the calculated 0_3^+ and 0_4^+ states are consistent with the corresponding observed values 9.04 MeV and 10.56 MeV of the experimental 0_3^+ and 0_4^+ states, respectively.

Next, we show some detailed features of the wave functions of these excited states obtained with $R_{\rm cut}=6$ fm. The GCM energies, rms radii, and the monopole matrix elements are calculated as shown in Fig. 2. Based on the R-matrix theory [29], the main partial α-decay widths into ^{8}Be(0^+) for the 0_2^+, 0_3^+, and 0_4^+ states are calculated to be 7.39 eV, 0.92 MeV, and 0.66 MeV, respectively, which agree with the experimental values 8.5 eV, 1.45 MeV, and 1.42 MeV for these three excited states. The adopted decay energies measured from the decay threshold by which we calculate penetrability factors are taken from experiments. The chosen channel radii are 5.5 fm, 10.0 fm, and 4.0 fm, respectively, which give the

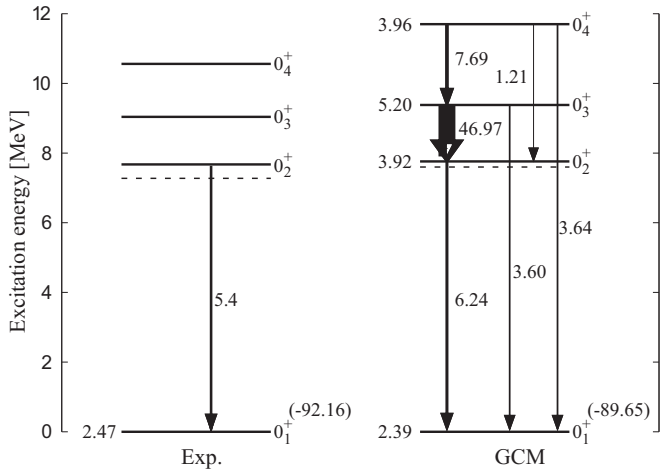

FIG. 2. The GCM energy levels, rms radii for the mass distributions (left side of the energy levels), and the monopole transition strengths (along the transition lines) for the ground state and excited 0^+ states in ^{12}C. The dashed lines are corresponding to the threshold energies. It should be noted that the observed radius for the ground state of ^{12}C from experiment is charge radius and it is from Ref. [28].

largest reduced width amplitudes around these points. Thus, the observed data of the 0_3^+ and 0_4^+ states are reproduced by our GCM calculations. It can be seen that the obtained 0_3^+ state has a very large radius, more than 5 fm, which is much larger than the gas-like Hoyle state. The calculated monopole strength between 0_2^+ and 0_3^+ of ^{12}C is about 47 e^2fm^4, which is much larger than other monopole transitions. This shows that the broad 0_3^+ state has more dilute density compared with the Hoyle state and we consider that the 0_3^+ state is a kind of breathing excited state of the Hoyle state as we discuss later.

Based on the orthogonality between the 0_1^+ state and 0_2^+ state of ^{12}C, a single orthogonalized THSR wave function of 0_2^+ state can be constructed as $\hat{\Phi}^{0_2^+}_{2\alpha+\alpha}(\boldsymbol{\beta}_1,\boldsymbol{\beta}_2) = (1-n_1|\hat{\Phi}^{0_1^+}_{\rm min}\rangle\langle\hat{\Phi}^{0_1^+}_{\rm min}|)\hat{\Phi}^{0^+}(\boldsymbol{\beta}_1,\boldsymbol{\beta}_2)$. Here, n_1 is a normalization factor and $\hat{\Phi}^{0_1^+}_{\rm min}(\beta_{1x}=0.1,\beta_{1z}=2.3,\beta_{2x}=2.8,\beta_{2z}=0.1)$ is the single optimum THSR wave function obtained by variational calculations, which is about 98% equivalent to the GCM ground wave function [24]. Thus, the optimum 0_2^+ THSR wave function $\hat{\Phi}^{0_2^+}_{\rm min}$ can be obtained with the minimum energy $E^{0_2^+}_{\rm min}(\beta_{1x}=4.9,\beta_{1z}=2.9,\beta_{2x}=10.7,\beta_{2z}=0.4) = -81.79$ MeV, which has a 98.3% squared overlap with the corresponding GCM solution. In the same way, we can construct a single orthogonalized THSR wave function of 0_3^+ by using the 0_1^+ and 0_2^+ wave functions, $\hat{\Phi}^{0_1^+}_{\rm min}$ and $\hat{\Phi}^{0_2^+}_{\rm min}$, namely $\hat{\Phi}^{0_3^+}_{2\alpha+\alpha}(\boldsymbol{\beta}_1,\boldsymbol{\beta}_2) = (1-n_1|\hat{\Phi}^{0_1^+}_{\rm min}\rangle\langle\hat{\Phi}^{0_1^+}_{\rm min}| - n_2|\hat{\Phi}^{0_2^+}_{\rm min}\rangle\langle\hat{\Phi}^{0_2^+}_{\rm min}|)\hat{\Phi}^{0^+}(\boldsymbol{\beta}_1,\boldsymbol{\beta}_2)$. This $\hat{\Phi}^{0_3^+}_{2\alpha+\alpha}(\boldsymbol{\beta}_1,\boldsymbol{\beta}_2)$ wave function provides us with another independent and simple way for confirming the existence of the 0_3^+ state in ^{12}C.

Figure 3 shows the contour plot for the energy of the 0_3^+ state as a function of spherical $\boldsymbol{\beta}_1$ and $\boldsymbol{\beta}_2$ calculated by using the wave function $\hat{\Phi}^{0_3^+}_{2\alpha+\alpha}(\boldsymbol{\beta}_1,\boldsymbol{\beta}_2)$. The two local minimum points, -79.83 MeV and -79.63 MeV, appear in the contour plot and they are connected by a flat valley. The squared

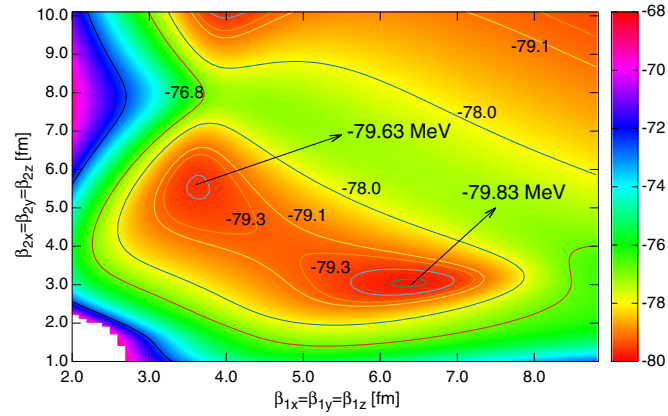

FIG. 3. The contour plot for the 0_3^+ state in the spherical $\boldsymbol{\beta}_1$ and $\boldsymbol{\beta}_2$ parameter space, which is obtained from the variation calculations of a constructed single THSR wave function orthogonalized to the ground and Hoyle states of ^{12}C.

overlap between these two states, $|\langle\hat{\Phi}^{0_3^+}_{\rm min1}(\beta_1=6.4,\beta_2=3.0)|\hat{\Phi}^{0_3^+}_{\rm min2}(\beta_1=3.6,\beta_2=5.6)\rangle|^2 = 0.840$, shows these two wave functions are not so close compared with the case of the contour plot for the Hoyle state [27]. Above the second local minimum point, we have checked that there is a quite large deep region, which belongs to the 3α continuum region and there are no local minimum points. Furthermore, the first local minimum energy -79.83 MeV is very close to the GCM energy -80.27 MeV for the 0_3^+ state. Most importantly, it is found that the squared overlap between this simple wave function $\hat{\Phi}^{0_3^+}_{\rm min1}$ and the GCM 0_3^+ wave functions, $|\langle\hat{\Phi}^{0_3^+}_{\rm min1}(\beta_1=6.4,\beta_2=3.0)|\hat{\Phi}^{0_3^+}_{\rm GCM}\rangle|^2$, is as high as 0.903. If we adopt the deformed THSR wave function, we can find an even better wave function and their squared overlap $|\langle\hat{\Phi}^{0_3^+}_{2\alpha+\alpha}(\beta_{1x}=6.7,\beta_{1z}=4.7,\beta_{2x}=4.1,\beta_{2z}=1.3)|\hat{\Phi}^{0_3^+}_{\rm GCM}\rangle|^2 = 0.944$. This high squared overlap indicates that the obtained orthogonalized THSR wave function $\hat{\Phi}^{0_3^+}_{2\alpha+\alpha}$ for the local minimum energy $E_{\rm min} = -79.8$ MeV is just the 0_3^+ orthogonalized THSR wave function of ^{12}C. Thus, we can say that the existence of the 0_3^+ state is confirmed again using the simple single 0_3^+ THSR wave function orthogonalized to the ground and Hoyle states.

Next, using the obtained GCM wave functions, we will investigate further the $\alpha + {}^8$Be correlation of the excited 0^+ states in ^{12}C. Here, we focus on the domain channel $[{}^8{\rm Be}(0^+)+\alpha]_{0^+}$ for the ground and excited 0^+ states in ^{12}C. We calculate the α RWA $\mathcal{Y}(a)$ defined as

$$\mathcal{Y}(a) = \sqrt{\frac{12!}{4!8!}}\left\langle\left[\hat{\Phi}^{0^+}_{2\alpha}, Y_{00}(\hat{\boldsymbol{\xi}}_2)\right]_{00}\frac{\delta(\xi_2-a)}{\xi_2^2}\phi(\alpha)\middle|\hat{\Phi}^{0_k^+}_{\rm GCM}\right\rangle. \quad (3)$$

Here, the normalized projected ^{8}Be THSR wave function is $\hat{\Phi}^{0^+}_{2\alpha} \propto P^{0^+}_{00}\mathcal{A}[e^{-\frac{\xi_{1x}^2}{B_x^2}-\frac{\xi_{1y}^2}{B_y^2}-\frac{\xi_{1z}^2}{B_z^2}}\phi^2(\alpha)]$. $B_k^2 = b^2+\beta_k^2$. In the RWA calculations, $\beta_x=\beta_y=3.0$ fm and $\beta_z=11.1$ fm, with which this 2α projected THSR wave function gives minimum energy by the use of the same interaction parameters of ^{12}C.

Figure 4 shows $\mathcal{Y}(a)$ for the four 0^+ states ($0^+_1 \sim 0^+_4$). It should be noted that, due to the optimized basis using one-by-one method in GCM, we got better and more extended wave functions for the excited 0^+ states in ^{12}C. We can see that the 0^+_3 state has a much larger extension compared with the Hoyle state. Since the number of nodes of the 0^+_3 state is larger by one than that of the Hoyle state, the 0^+_3 state can be considered as an excited state of the Hoyle state at least for 2α-α part, which have also been discussed in Refs. [10,15]. On the other hand, the reduced width amplitude of the 0^+_4 state for the channel $^8\mathrm{Be}(0^+)+\alpha$ is much smaller than that of the 0^+_3 state, which implies that the $^8\mathrm{Be}(0^+)+\alpha$ component of the 0^+_4 state is much smaller than that of the 0^+_3 state. This fact is consistent with the bent-arm structure of the 0^+_4 state.

Another essential problem is how about the 2α behaviors in these excited states. To study the 2α correlation in the excited 0^+ states in ^{12}C, we introduce the following 2α relative wave function of ^{12}C:

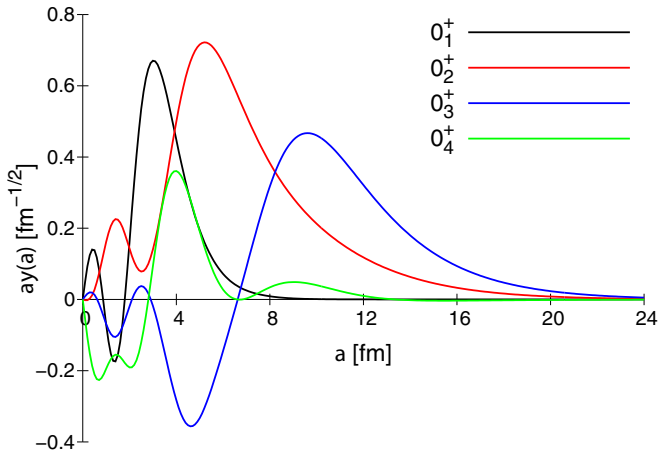

FIG. 4. The α reduced width amplitudes of the 0^+_1,0^+_2,0^+_3, and 0^+_4 states for the $[^8\mathrm{Be}(0^+)+\alpha]_{0^+}$ channel in ^{12}C.

$$\chi(a) = N_0\sqrt{\frac{12!}{4!4!4!}}\left\langle\left[e^{-\frac{\xi_{2x}^2}{B_{2x}^2}-\frac{\xi_{2y}^2}{B_{2y}^2}-\frac{\xi_{2z}^2}{B_{2z}^2}}\phi^3(\alpha)\right]^{0^+}\frac{\delta(\xi_1-a)}{\xi_1^2}Y_{00}(\hat{\boldsymbol{\xi}}_1)\middle|\hat{\Phi}^{0^+_k}_{\mathrm{GCM}}\right\rangle. \tag{4}$$

Here, N_0 is the normalization factor $N_0 = 1/\langle[e^{-\frac{\xi_{2x}^2}{B_{2x}^2}-\frac{\xi_{2y}^2}{B_{2y}^2}-\frac{\xi_{2z}^2}{B_{2z}^2}}\phi^3(\alpha)]^{0^+}|[e^{-\frac{\xi_{2x}^2}{B_{2x}^2}-\frac{\xi_{2y}^2}{B_{2y}^2}-\frac{\xi_{2z}^2}{B_{2z}^2}}\phi^3(\alpha)]^{0^+}\rangle$. $\chi(a)$ is the relative wave function between two α clusters inside ^{12}C. $B_{2k}^2 = \frac{3}{4}b^2+\beta_{2k}^2$ and their values are chosen as follows.

To choose some typical values of the parameter $\boldsymbol{\beta}_2$ in Eq. (4), we firstly search for the largest squared overlaps between the single THSR wave functions and the 0^+ GCM wave functions. As for the ground state, we have known that the obtained $\hat{\Phi}^{0^+_1}_{\mathrm{min}}(\beta_{1x}=0.1,\beta_{1z}=2.3,\beta_{2x}=2.8,\beta_{2z}=0.1)$ wave function by variational calculations almost gave the largest squared overlap, 0.978, with the GCM ground wave function. The obtained largest squared overlaps for the excited 0^+ states are $|\langle\hat{\Phi}^{0^+}(\beta_{1x}=9.3,\beta_{1z}=4.6,\beta_{2x}=7.2,\beta_{2z}=0.1)|\hat{\Phi}^{0^+_2}_{\mathrm{GCM}}\rangle|^2_{\mathrm{max}}=0.837$; $|\langle\hat{\Phi}^{0^+}(\beta_{1x}=9.3,\beta_{1z}=9.2,\beta_{2x}=13.8,\beta_{2z}=13.7)|\hat{\Phi}^{0^+_3}_{\mathrm{GCM}}\rangle|^2_{\mathrm{max}}=0.290$; $|\langle\hat{\Phi}^{0^+}(\beta_{1x}=0.7,\beta_{1z}=9.2,\beta_{2x}=0.7,\beta_{2z}=7.7)|\hat{\Phi}^{0^+_4}_{\mathrm{GCM}}\rangle|^2_{\mathrm{max}}=0.446$. These obtained largest single THSR wave function components show that there are possibly very different intrinsic shapes in these excited states in ^{12}C. For example, the largest component wave function in 0^+_3 GCM wave function, $\hat{\Phi}^{0^+}(\beta_{1x}=9.3,\beta_{1z}=9.2,\beta_{2x}=13.8,\beta_{2z}=13.7)$, has very large and nearly spherical size parameters $\boldsymbol{\beta}_1$ and $\boldsymbol{\beta}_2$, which reflect the large-radius character of the 0^+_3 state. The largest single wave function component in 0^+_4 GCM wave function has a very obvious deformed prolate intrinsic shape, which indicates the possible rigid bent-arm structures of 0^+_3 state obtained from AMD and FMD.

To study the 2α correlations of the four 0^+ states in ^{12}C in different situations, four sets of values of the parameter $\boldsymbol{\beta}_2$ in Eq. (4) are adopted from the above obtained single THSR wave functions. Figure 5 shows 2α correlation functions of the 0^+_1,0^+_2,0^+_3, and 0^+_4 states in ^{12}C using different obtained values of $\boldsymbol{\beta}_2$ parameters. It is the first time that the 2α behaviors are calculated in these 0^+ states in ^{12}C. Due to Pauli principle between 2α clusters, in the internal region, the 2α correlation functions have two nodes and they are located at almost the same positions, namely about 1 fm and 2 fm, even for the different 0^+ states. In the outside region, the 2α correlations in these states display some complicated behaviors and how to understand this kind of correlation is the subject of a forthcoming paper. Here, we only need to emphasize that, in the 2α correlation function, for the 0^+_3 state, it has much more extended tail part and also has one more node than the Hoyle state in some sense. It should be noted that, as for Fig. 5(c), the 0^+_3 state still can be considered to have some "node" in outside region of 4 fm $\leqslant a \leqslant$ 8 fm, which has a similar situation with the Hoyle state in Fig. 4 in the region of 2 fm $\leqslant a \leqslant$ 4 fm. This shows that, compared with the Hoyle state, the 0^+_3 state is not only excited from the 2α-α part but also from the 2α correlation part.

Now, we clarify further the underlying physical meaning of the number of nodes of 2α-α and α-α relative wave functions for the 0^+_3 state in ^{12}C. As we know, the operator which generates the breathing excitation is just the squared radius operator O_B as follows:

$$O_B = \sum_{i=1}^{12}(\boldsymbol{r}_i - \boldsymbol{r}_{\mathrm{c.m.}})^2. \tag{5}$$

This O_B is nothing but the operator of monopole transition and it also can be rewritten as

$$O_B = \sum_{k=1}^{3}\sum_{i\in\alpha_k}(\boldsymbol{r}_i - \boldsymbol{X}_k)^2 + 2\xi_1^2 + \frac{8}{3}\xi_2^2, \tag{6}$$

where $\boldsymbol{X}_k$ is the center-of-mass coordinate of the kth α cluster. The breathing excitation by $\boldsymbol{\xi}_2$ coordinate increases the number of nodes of the relative wave function between 2α and α, while the breathing excitation by $\boldsymbol{\xi}_1$ coordinate increases the

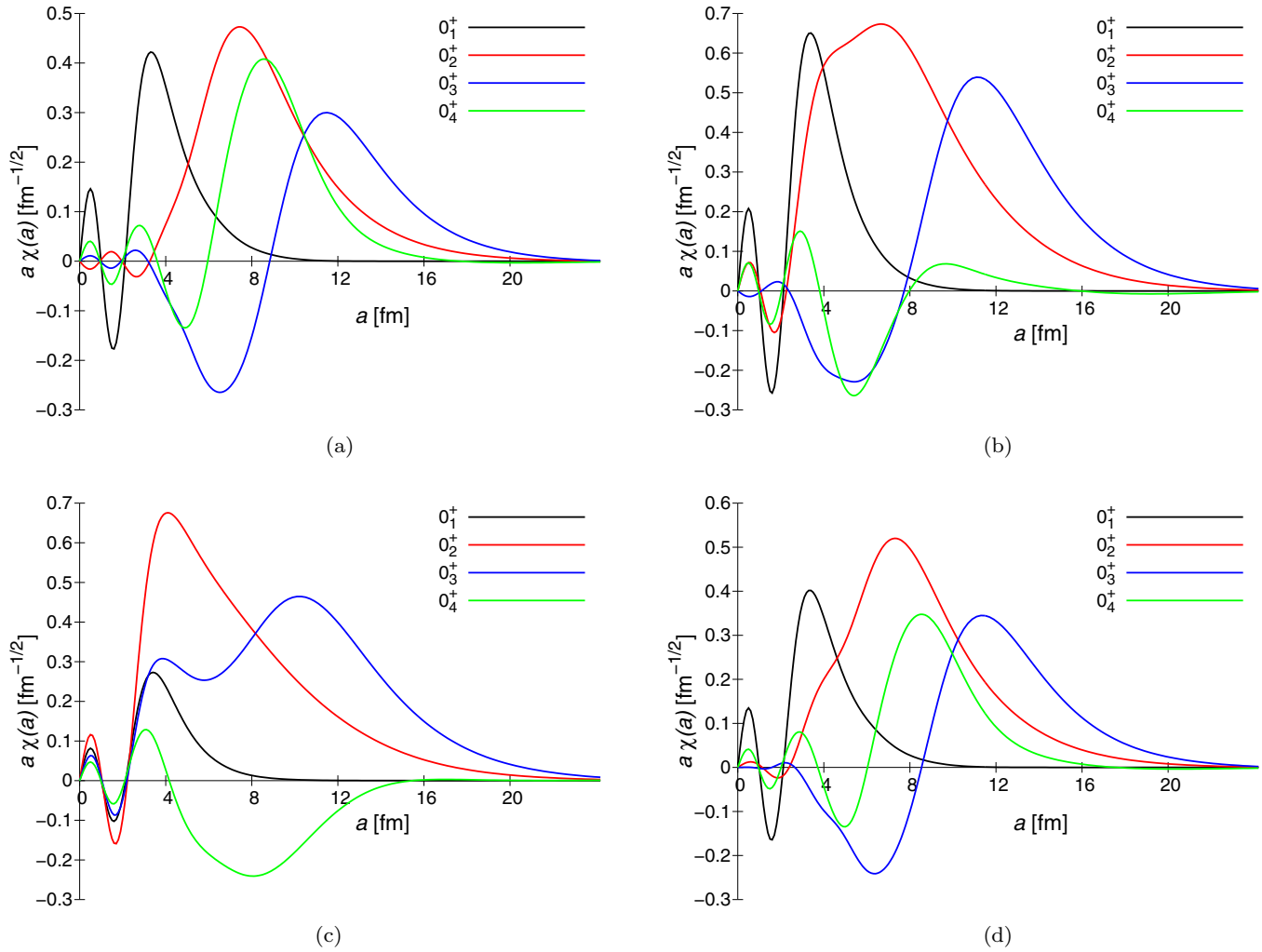

FIG. 5. The calculated 2α correlation wave functions of the 0_1^+,0_2^+,0_3^+, and 0_4^+ states using four sets of $\boldsymbol{\beta}_2$ parameters in ^{12}C. (a) (β_{2x}, β_{2z}) = (2.8 fm,0.1 fm). (b) (β_{2x}, β_{2z}) = (7.2 fm,0.1 fm). (c) (β_{2x}, β_{2z}) = (13.8 fm,13.7 fm). (d) (β_{2x}, β_{2z}) = (0.7 fm,7.7 fm).

number of nodes of the relative wave function between α and α. Therefore the breathing excitation is caused by both $\boldsymbol{\xi}_1$ and $\boldsymbol{\xi}_2$ coordinates. The 2α-α relative wave function, namely RWA of ^{12}C has been discussed for a long time, including the recent work done by Funaki [15]. However, regarding the 0_3^+ state as a breathing-like excited state of the Hoyle state, we have to study also the α-α relative wave function. In our present paper we investigated, for the first time, the α-α relative wave function. When we investigate the number of nodes of relative wave functions of $\boldsymbol{\xi}_2$ and $\boldsymbol{\xi}_1$, we should be careful about the following point. For example, when we study the number of nodes of the relative wave function of $\boldsymbol{\xi}_2$, the relative wave function of $\boldsymbol{\xi}_1$ should be kept nonexcited. The RWA which is the relative wave function of $\boldsymbol{\xi}_2$ is calculated by using the ground-state wave function of ^{8}Be for integrating out with respect to $\boldsymbol{\xi}_1$. Similarly in calculating the α-α relative wave function in Eq. (4), we used a nonexcited relative wave function of $\boldsymbol{\xi}_2$, namely the simple Gaussian function of $\boldsymbol{\xi}_2$. The calculated results for 2α-α and α-α wave functions in Figs. 4 and 5 both show that the obtained 0_3^+ state can be considered to have one more node than the Hoyle state. This means that the 0_3^+ state is not only excited from the 2α-α part but also from 2α correlation part. Considering the very large monopole transition from 0_3^+ state to Hoyle state, therefore, we think this confirmed 0_3^+ state is a breathing-like mode of the Hoyle state.

In summary, the existence of the 0_3^+ and 0_4^+ states in ^{12}C is confirmed by using an improved THSR-GCM with the radius-constraint method. The existence of the 0_3^+ state is also well supported by variational calculations using the single 0_3^+ THSR wave function orthogonalized to the ground and Hoyle states. Moreover, we found that the 0_3^+ state has a very large radius and there is a very large monopole transition from this state to the Hoyle state. By showing the RWAs and 2α correlation functions, we found that the 0_3^+ state is excited from both the 2α-α part and 2α correlation part of the Hoyle state. We concluded that the 0_3^+ state is a breathing-like excited state of the Hoyle state.

ACKNOWLEDGMENTS

The authors would like to thank Prof. Gerd Röpke, Prof. Peter Schuck, Prof. Taiichi Yamada, Prof. Yasuro Funaki, and Prof. Chang Xu for helpful discussions. B.Z. is grateful to the fruitful discussions with Prof. Masaaki Kimura and other members of the nuclear theory group in Hokkaido University. Numerical computation in this work was carried out at the Yukawa Institute Computer Facility. This work was supported by the National Natural Science Foundation of China (Grants No. 11535004, No. 11375086, and No. 11120101005) and also by JSPS KAKENHI Grant No. 16K05351.

[1] N. Moiseyev, *Non-Hermitian Quantum Mechanics* (Cambridge University Press, Cambridge, 2011).
[2] Z. Ren, C. Xu, and Z. Wang, Phys. Rev. C **70**, 034304 (2004).
[3] D. Ni and Z. Ren, Phys. Rev. C **87**, 027602 (2013).
[4] C. Xu, Z. Ren *et al.*, Phys. Rev. C **93**, 011306(R) (2016).
[5] S. Aoyama, T. Myo *et al.*, Prog. Theor. Phys. **116**, 1 (2006).
[6] M. Freer and H. O. U. Fynbo, Prog. Part. Nucl. Phys. **78**, 1 (2014).
[7] M. Itoh, H. Akimune, M. Fujiwara *et al.*, Phys. Rev. C **84**, 054308 (2011).
[8] W. R. Zimmerman, M. W. Ahmed *et al.*, Phys. Rev. Lett. **110**, 152502 (2013).
[9] M. Freer, S. Almaraz-Calderon *et al.*, Phys. Rev. C **83**, 034314 (2011).
[10] E. Uegaki, Y. Abe, S. Okabe, and H. Tanaka, Prog. Theor. Phys. **62**, 1621 (1979).
[11] Y. Kanada-En'yo, Prog. Theor. Phys. **117**, 655 (2007).
[12] M. Chernykh, H. Feldmeier, T. Neff, P. von Neumann-Cosel, and A. Richter, Phys. Rev. Lett. **98**, 032501 (2007).
[13] C. Kurokawa and K. Kato, Phys. Rev. C **71**, 021301(R) (2005).
[14] S.-I. Ohtsubo, Y. Fukushima, M. Kamimura, and E. Hiyama, Prog. Theor. Exp. Phys. (2013) 73D02.
[15] Y. Funaki, Phys. Rev. C **92**, 021302(R) (2015).
[16] H. Horiuchi, Prog. Theor. Phys. Suppl. **62**, 90 (1977).
[17] A. Volkov, Nucl. Phys. **74**, 33 (1965).
[18] A. Tohsaki-Suzuki, M. Kamimura, and K. Ikeda, Prog. Theor. Phys. Suppl. **68**, 359 (1980).
[19] Y. Fujiwara, H. Horiuchi *et al.*, Prog. Theor. Phys. Suppl. **68**, 29 (1980).
[20] A. Tohsaki, H. Horiuchi, P. Schuck, and G. Röpke, Phys. Rev. Lett. **87**, 192501 (2001).
[21] B. Zhou, Y. Funaki, H. Horiuchi, Z. Ren *et al.*, Phys. Rev. C **89**, 034319 (2014).
[22] Y. Funaki, H. Horiuchi, and A. Tohsaki, Prog. Part. Nucl. Phys. **82**, 78 (2015).
[23] B. Zhou, Y. Funaki, H. Horiuchi, Z. Ren *et al.*, Phys. Rev. Lett. **110**, 262501 (2013).
[24] B. Zhou, Y. Funaki, A. Tohsaki, H. Horiuchi, and Z. Ren, Prog. Theor. Exp. Phys. (2014) 101D01.
[25] Y. Funaki, H. Horiuchi, and A. Tohsaki, Prog. Theor. Phys. **115**, 115 (2006).
[26] M. Kamimura, Nucl. Phys. A **351**, 456 (1981).
[27] Y. Funaki, A. Tohsaki, H. Horiuchi, P. Schuck, and G. Röpke, Phys. Rev. C **67**, 051306(R) (2003).
[28] H. De Vries, C. W. De Jager, and C. De Vries, At. Data Nucl. Data Tables **36**, 495 (1987).
[29] A. M. Lane and R. G. Thomas, Rev. Mod. Phys. **30**, 257 (1958).